International Journal of Advanced Multidisciplinary Research
ISSN: 2393-8870
www.ijarm.com
(A Peer Reviewed, Referred, Indexed and Open Access Journal)
DOI: 10.22192/ijamr Volume 9, Issue 10 -2022

Research Article

DOI: http://dx.doi.org/10.22192/ijamr.2022.09.10.001

# Discovery of New Remdesivir Analogs against Main Protease ($M^{pro}$) & RNA-Dependent RNA polymerase (RdRp) Targets of SARS-CoV-2: Molecular Docking, Physicochemical Properties, and Structure-Activity Relationship Studies

**Babasaheb V Kendre[1]*, Pawan S Hardas[1], Rushikesh B Kendre[2]**
[1]Post Graduate Research Centre in Chemistry, Vaidyanath College, Parli-Vaijnath-431515, Dist. Beed, MS, India
[2]Maharashtra Institute of Medical Sciences and Research, Latur-413512, MS, India
*Corresponding Author: *bvkendre71@gmail.com*

**Keywords**

SARS-CoV-2, Coronavirus, Molecular Docking, COVID-19, RdRp, $M^{pro}$, Ascorbic acid, SARs, ADMET, physicochemical properties.

## Abstract

Two and half-years back, the people from Wuhan, China, have experienced the accidental outbreak of SARS-CoV-2 thereafter the waves of coronaviruses are intensely dominating the world's population claiming more than 5,785,438 deaths out of 401,987,142 infected cases as of 9 February, 2022. More importantly, the different countries have lost millions of rupees to combat the critical situation. Recently, two antiviral drugs namely paxlovid and molnupiravir were approved to treat SARS-CoV-2 infections. Antiviral, antimalarial and anti-inflammatory drugs in combination with immunity building vitamins have been extensively used in the therapy to recover hospitalized patients. Recently, the vaccination drive has given somewhat relief to the human community. However, the emergence of new variants has started dominating to the human life globally. In current therapy, remdesivir is one of the drugs which have showed significant recovery rates for critically ill patients. However, remdesivir is not too safe to use for its serious side effects. Therefore, there is an urgent demand of new therapeutics holding significant efficacy profile to control this critical situation. Working on the similar lines, we have designed a library of new antiviral therapeutics analogous to remdesivir for the treatment of coronavirus infections. As per the literature reports, RNA-dependent RNA polymerase (RdRp) is an attractive target for antiviral drugs. In addition, $M^{pro}$ is a key enzyme of coronaviruses that plays an essential role in mediating viral replication and transcription process. Firstly, the crystal structures of viral protein (PDB ID 6LU7) & (PDB ID: 6M71) was retrieved from the RCSB Protein Data Bank. Computer-Aided Drug Design (CADD) and molecular docking (MD) studies were performed for the identification of new drugs.

The molecular docking results of a library of molecules were compared with the results of remdesivir for identifying the best drug candidate against COVID-19. Molecular docking study reveals that a lead molecule, 15 showed strong intermolecular interactions with the key residues (Asp760, Asp623, Lys621, Tyr455, Lys551 & Arg553) of RdRp offering XP Glide Gscore -8.045kcal/mol. The intermolecular interactions of the same molecule with the key residues of $M^{pro}$ include Gln189, His164, Glu166 and Phe140 along with XP Glide Gscore -5.813kcal/mol. The predicted ADMET values for a lead molecule as well as all molecules in a series were quite satisfactory and follow Lipinski's rule of five.

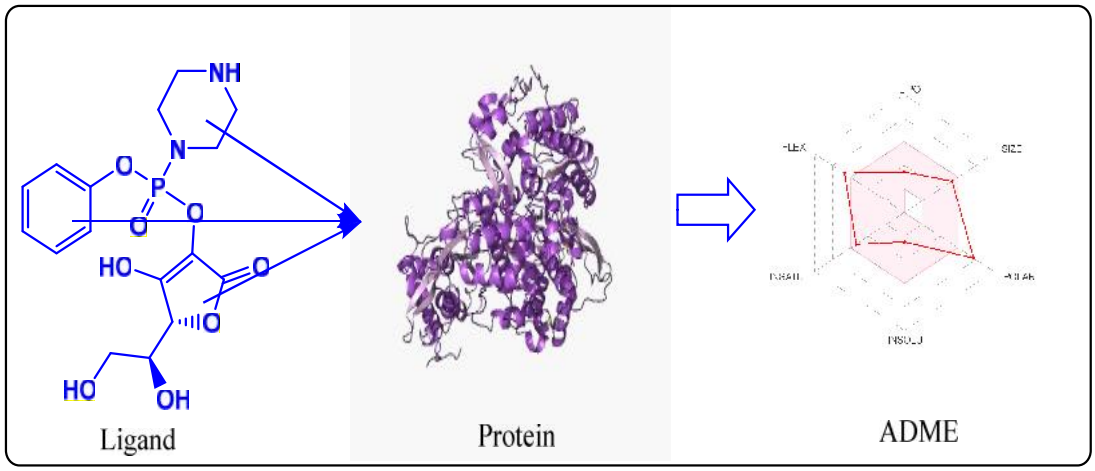


**Figure A:** Novel inhibitor of SARS-CoV-2

## Introduction

Viruses are continuously in the spotlight from the past few decades as they intensely threat human population by means of acute and chronic infections. In the current pandemic situation, mutation in coronavirus is a significant issue. The second massive wave was too much devastating that claimed millions of deaths [Long et al., 2020]. Coronaviruses is prone to genetic structural changes. The emerging coronaviruses such as omicron and delta have high rates of human to human transmission as compared to the late 2019 virus [Garvin et al., 2020]. For these reasons, ongoing vaccination drive is not entirely successful. As a result, the death figures are continuously rising with huge economic expenses. In order to combat this critical situation, there is urgent call for the discovery of potential therapeutics as drugs is a lifeline for hospitalized patients.

The human history records most dangerous pandemics during 430 B.C. to 2019, of them plague and cholera have claimed highest deaths [Council et al., 2020]. The outbreaks of MERS & SARS had relatively low mortality rates of human population [Huremović et al., 2019]. The second wave of SARS-CoV-2 was become a super killer that records high deaths (2,692,621) around the world as of 15th March, 2021 [https://www.worldometers.info/coronavirus/access 2021]. Necessary steps including quarantine, mobility & travelling restrictions, compulsory masking, PPE for paramedical staffs, social distancing, lockdowns, awareness initiatives, COVID-19 apps, vaccination drive, etc. were taken by the government for prevention of community transmission. Earlier in December 2019, the outbreak of pneumonia in Wuhan, China, forced researcher to identify the reasons of infections [Lu et al., 2020; Zhu et al., 2020]. During research studies, a novel strain of coronavirus (2019-nCoV) was detected.

It was further designated as severe acute respiratory syndrome i.e. SARS-CoV-2 by International Committee on Virus Taxonomy (ICVT) [Coronaviridae Study Group of the International Committee on Taxonomy of Viruses]. Many studies reveal that the eruption of viruses including HCoV-NL63 in 2004, SARS-CoV (Severe Acute Respiratory Syndrome) in 2002, MERS-CoV (Middle East Respiratory Syndrome) in 2003, and SARS-CoV-2 in 2019 have zoonotic origin [van der Hoek etal., 2004; Gu et al., 2007; de Groot et al.; 2013].

Following the outbreaks of SARS-CoV-2 infections, different countries undertaken clinical trials of existing therapeutics including chloroquine & hydroxychloroquine, lopinavir, dharunavir, favipiravir, remdesiviretc, which were earlier approved by FDA against malaria, HIV, influenza virus, pneumonia and some other types of infections [Singh et al., 2020]. Remdesivir is the only one drug in wide use that targets RdRp enzyme responsible for viral replications. Despite the tremendous advances in antiviral therapeutics and understanding of virus-host relationship, existing and emerging viral diseases remains a challenging problem. The major clinical issue is antiviral resistance while treating patients suffering through viral and chronic diseases. The reasons for increasing resistance are the accumulation of mutations in the viral genome [Peck et al., 2018].

Nowadays, there is growing interest over the use of natural sources, in particular the plant and animal kingdom for the discovery of potential drugs through virtual drug design and molecular docking techniques [Dehelean et al., 2021, Rathor et al., 2021, Veeresham et al., 2012]. The role of vitamins is crucial for maintaining human health as different vitamins play different roles in the body. They are essential nutrients to stay healthy. In short, vitamins are immunity builders and they are able to fight against several types of infections [Maqbool et al., 2017]. The viral infection occurs when there is attachment of spike (S) glycoprotein to human cell receptor angiotensin-converting enzyme 2 (ACE-2). At the SARS-CoV-ACE2 interface, two virus binding hotspots were previously identified [Wu et al., 2012]. A hotspot Lys31 consists of a salt bridge between Lys31 and Glu35 and another hotspot Lys353 consists of a salt-bridge between Lys353 and Asp38. The molecular docking study reveals that some vitamins have good tendency to act at the interface of spike S and ACE2 (Figure B (a)). If the person has a balanced diet with daily exercise, it can help to boost immunity to protect from viral infections. Ascorbic acid, commonly called as vitamin C is an essential vitamin possesses antiviral properties [Hemilä 2017]. It is a potent antioxidant. There is also growing interest for the administration of vitamin C for the patients under malnourished conditions [Carr et al., 2017]. A study suggested that there are several health benefits for the patients suffering through severe sepsis and septic shock [Kuhn et al., 2018]. There were many misconceptions over the use of vitamin C, which was ruled out by Nobel Laureate Linus Pauling [Pauling 1971; Pauling et al., 1991]. The several research papers on the potential benefits of the vitamin C in the treatment of viral infections have been published [Biancatelli et al., 2020].

There are hundreds of viruses that cause respiratory infections, out of them several are coronaviruses. It is very difficult to have drug treatment for each class of viral infection because each is individualized and drug development is very expensive [Richman 2016]. There is no specific drug ever found to be safe and effective for the treatment of COVID-19. The current treatment includes supportive care, i.e., oxygen therapy, fluid management, use of approved antiviral drugs developed for Ebola (remdesivir), anti-HIV (lopinavir, ritonavir), and recently approved antimalaria drugs (hydroxychloroquine) as a combination therapy (Figure B (b)). The combination of azithromycin and hydroxychloroquine was also shown as a partial treatment against COVID-19. As of 5 April, 2021, more than twelve vaccines including Comirnaty (BNT162b2), Moderna COVID-19 Vaccine (mRNA-1273), COVID-19 Vaccine (AZD1222) also known as Covishield, Sputnik V, COVID-19 Vaccine Janssen (JNJ-78436735; Ad26.COV2.S), Corona Vac, BBIBP-CorV, EpiVacCorona,

Convidicea (Ad5-nCoV) and Covaxin have now been authorized all around the world and many more are under development [Belete 2021].

More importantly, collective and multidisciplinary efforts are needed to develop specific therapeutics to effectively inhibit two key enzymes of SARS-CoV-2 including PDB: 6LU7 and PDB: 6M71 respectively [Iftikhar et al., 2020]. The recent research studies reveal that SARS-CoV-2 S RBD has very high binding affinity with hACE2 than SARS-CoV [Wan et al., 2020]. A study highlights that the residues of 6LZG including GLN493 and GLU484 form intermittent interactions with hotspot Lys31 of ACE2. The probability of interaction between GLN493 and hotspot Lys31 was recently reported [Lan et al., 2020]. The simulation study also emphasizes on the sustainable interactions of Gly502 and Gln498 with the residue Lys353 of ACE2. It is noteworthy to mention that the residues Gln493 and Gln498 of SARS-CoV-2 form sustainable interaction with Glu35 and Asp38 of ACE2, respectively.

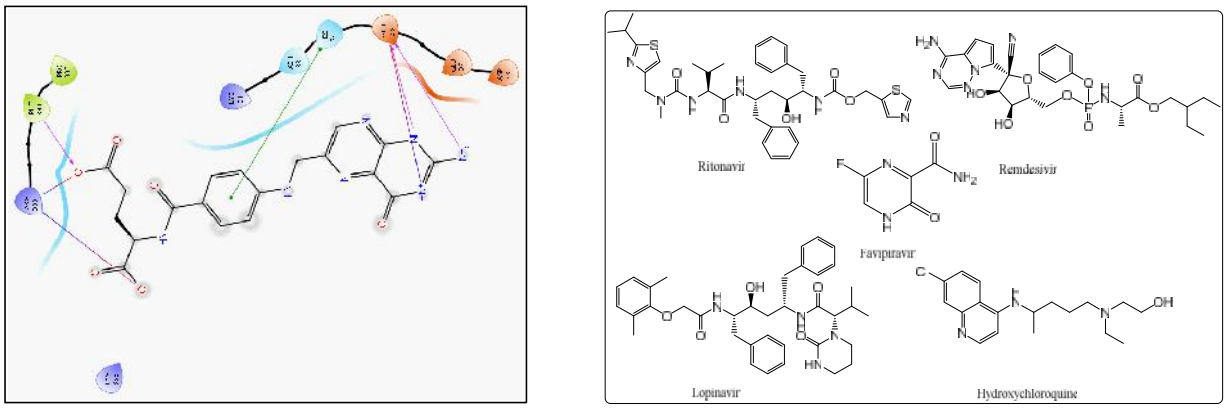


(a) (b)

**Figure B**: (a) Molecular interactions of folic acid at the interface of spike (s) glycoprotein-ACE2 receptor (PDB ID 2AJF); (b) Approved antiviral drugs.

## Materials and Methods

The protease structure, the 3-chymotrypsin-like cysteine protease (3CLpro) enzyme of SARS-CoV-2 (PDB ID: 6LU7) with 2.1 Å & the crystal structure of viral protein (PDB ID: 6M71) were retrieved from the RCSB Protein Data Bank (http://www.rcsb.org). The computational work was performed using Schrödinger software.

**2.1. Preparation of Protease Structures.** The SARS-CoV-2 virus protein structures were prepared in the Protein Preparation Wizard and Prime module of the Schrödinger suite to remove defects such as missing hydrogen atoms, inappropriate bond order assignments, charge states, alignments of several groups, and missing side chains [Protein Preparation Wizard 2020; Prime 2020]. Steric hindrance and strained bonds/angles were removed through restrained energy minimization, permitting movement in heavy atoms up to 0.3 Å.

**2.2. Virtual Screening of FDA Approved Drugs.** FDA approved drugs such as remdesivir, ritonavir, paxlovid and molnupiravir were screened to select the hits as reference molecule or positive control for the design of novel compounds. The mol files of approved drugs were obtained from the Protein Data Bank at the RCSB site (http://www.rcsb.org) and PubChem [Yin et al., 2020; Jin et al., 2020].

More than1500 analogs were prepared by the Maestro tool. The structures of both approved antiviral drugs and a library of new remdesivir analogs were prepared prior to docking by Ligprep. Ligprep assisted the production of 2D or 3D structures and their corresponding low-energy

3D structures, which were immediately available for Glide program applications. All the parameters were kept as the default except chirality parameters for the antiviral drugs and new HEA analogs. The chirality was kept as the default for the 3D structures, and all the combinations of chirality were developed for the approved antiviral drugs and new remdesivir analogs. Next, desalting, tautomer generation, and probable ionization states at pH 7 ± 2 were adjusted. Ionization states of all the molecules were predicted by the Schrodinger suite inbuilt Epik module [LigPrep 2020, Epik 2020].

### 2.3. Molecular Docking of a Library of Compounds against Target Active Sites.

Target-specific molecular docking of approved drugs (Table 1) and a library of new drugs (Table 2) against two enzymes was accomplished using the Glide module of the Schrodinger suite. The Glide tool was used for receptor grid preparation at default parameters, which include a van der Waals radius scaling factor (1.0) and partial charge cutoff (0.25). The screening of both libraries was performed by Glide at extra precision (XP), which indicates an appropriate connection between excellent poses and good scores.

### 2.4. ADMET Calculations.

Swiss ADME and admetSAR online tools were employed to predict the ADMET (i.e., absorption, distribution, metabolism, excretion, and toxicity) profile of identified hit compounds (1-24) and two antiviral drugs (remdesivir and paxlovid) [Daina et al., 2017; Cheng et al., 2012]. The predicted ADMET properties include molecular weight, H-bond acceptor, H-bond donors, predicted octanol/water partition coefficient (MLogP), TPSA (total polar surface area), Lipinski (drug-likeness) and Rat LD50. The results are shown in Table 3.

## Results and Discussion

Since the detection of SARS-CoV-2 in Wuhan, China and its spreading all around the world, the tremendous efforts have been made not only regarding the identification of structure of coronavirus but also for the discovery of suitable medication to neutralize coronavirus infections. Most of the countries have developed their own vaccinations and undertaken clinical trials of available drugs. Very recently, the new treatments are recommended as the pandemic accelerates worldwide. The millions of new cases of COVID-19 were reported to the WHO in the last few weeks. Most of the cases are of omicron and delta variants. It has been recommended to use interleukin-6 receptor blockers (e.g., srilumab and tocilizumab) and systematic corticosteroids (e.g., dexamethasone) for patients with severe or critical COVID-19. The Food and Drug Administration recently authorized the use of new antiviral medication against omicron (e.g., paxlovid) developed by Pfizer and (molnupiravir) by Merck [Planas et al., 2022]. The Food and Drug Administration (FDA) issued an Emergency Use Authorization (EUA) on December 8, 2021, for the anti-SARS-CoV-2 monoclonal antibodies (mAbs) tixagevimab plus cilgavimab (Evusheld) [Food and Drug Administration, 2021]. The EUA allows this combination to be used as pre-exposure prophylaxis (PrEP) in certain individuals who, if infected, are at high risk of progressing to severe COVID-19. These mAbs are SARS-CoV-2 spike protein-directed attachment inhibitors that bind to nonoverlapping regions of the receptor binding domain of the SARS-CoV-2 spike protein. This combination of mAbs appears to have activity against the B.1.617.2 (Delta) variant.

Of particular note, finding a potent molecule with drug-like properties remains challenging, and therefore, advanced drug discovery involves CADD approaches that accelerates the early discovery phases. The main protease, $M^{pro}$, of SARS-CoV-2 was presented as an attractive drug target, and a rapid identification of drug

candidates was achieved through virtual screening. Encouraged with this, and exploiting a recently published crystal structure of $M^{pro}$ and RdRp from SARS-CoV-2 (PDB code 6LU7 and 6M71), we executed virtual screening for the 4 antiviral drugs. The list of the compounds is presented in Table 1.

### 3.1. Virtual Screening of Antiviral Drugs and New nucleotide analogues against SARS-CoV-2 Proteins $M^{pro}$ & RdRp.

Molecular docking of approved antiviral drugs was carried out with proteins $M^{pro}$ and RdRp using the Glide module of the Schrödinger suite, as these two were found to be an attractive drug targets for SARS-CoV-2. The main protease ($M^{pro}$) is a key enzyme of coronaviruses and has an essential role in mediating viral replication and transcription process. The RNA-dependent RNA polymerase is responsible to regulate viral replications [Strasfeld et al., 2010]. Encouraging with above facts, target based virtual screening and molecular docking of approved antiviral drugs and designed compounds was carried out in the present study. The poses of ligands were ranked according to Glide XP Gscore (kcal/mol). After docking with Mpro (PDB ID: 6LU7), the 4 antiviral drugs according to their XP Gscore were listed in the table **1**. Among them, paxlovid, the oral antiviral candidate for the treatment of COVID-19 investigated by Pfizer laboratories was realized as the best inhibitor of $M^{pro}$ showed Glide XP Gscore -7.620 kcal/mol (Table 1, entry 3). Remdesivir, an antiviral medication developed for the treatment of Ebola, secured rank second, was showed XP Gscore -6.974 kcal/mol (Table 1, Entry 2).The third rank was secured by molnupiravir, showed XP Gscore -6.406 kcal/mol, which is proposed therapeutic for the treatment of SARS-CoV-2 infections and found to inhibit the replication of certain RNA viruses (Table 1, Entry 4). However, when these drugs were docked with RdRp (PDB ID: 6M71), first and second ranks were secured by molnupiravir and remdesivir, showed XP GScores -6.295 & -4.942 kcal/mol respectively (Table 1, Entry 1 and 4). Our results were in agreement with the docking score of remdesivir (−7.804 kcal/mol) reported by Sumit Kumar and coworkers on Schrödinger software [Kumar et al, 2020]. Interactions of monupiravir with the Mpro and RdRp proteins are presented in Figure 3. Remdesivir, showed intermolecular interactions with the key residues Gln189, Thr190, Gly143, Glu166 and His41of $M^{pro}$ (PDB ID: 6LU7). On the other hand, remdesivir showed intermolecular interactions with the key residues Asp760, Asp618, Lys621, Asp623, and Arg553 of RdRp (PDB ID: 6M71). The above results indicate that remdesivir is an important pharmacophore to build a new library of nucleotide analogues that contains a sugar molecule, phosphate group and nitrogen containing base. Taking into account the effectiveness of remdesivir in the inhibition of RNA-polymerase, we propose herein a new library of nucleoside analogues to study their effectiveness against COVID-19 with improved efficiency and efficacy values.

The COVID-19 pandemic has led to massive loss of human life along with social and economic disruption worldwide that has posed unprecedented challenges before world's health system. These facts encouraged our research group for searching novel antiviral therapeutics using advanced tools and techniques. With the presence of nucleoside base in remdesivir and our ongoing research towards the identification of new nucleotide analogues, a small library of nucleotide compounds was designed and performed virtual screening against two proteins ($M^{pro}$ & RdRp). Out of 1500 screened new nucleoside analogues, top scoring 28 compounds were selected and listed in the tables 2 and 3 respectively.

In a new series, the top-ranked molecule (Table 2, entry 1) was showed the highest docking score (−9.648), free energy of binding -48.66 and ligand efficiency value -0.269 with protein (PDB ID: 6LU7). On the other hand, the molecular docking results of designed molecules with protein (PDB ID: 6M71) showed docking score -8.856, XP Gscore -9.116 kcal/mol and intermolecular interactions with top ranked molecule (Table 3, entry 1).

In the next step, we continued our study to evaluate all new molecules (25) along with two antiviral drugs (Paxlovid & Remdesivir) for their ADMET profile [Lipinski et al., 2004]. Testing of ADMET properties is very essential step for searching suitable drug candidate. After evaluating all molecules for ADMET properties, their results were entered in table 4 and compared with standard antiviral drugs. The screening results of all molecules showed that only two molecules (entry 15 & 22, Table 4) strictly follow the Lipinski's rule of five to meet drug-likeness properties. Most of the molecules (except 1, 5, 8, 16, 17, and 20) followed the criteria of rule with a slight deviation in number of rotatable bonds or molecular weight or number of hydrogen acceptors /donors. Tabular data shows that 20 molecules of 25 have molecular weights less than 500da, are capable to cross BBB through lipid mediated free diffusion. According to SwissADME method, a molecule with molecular weight between 150 to 500 g/mol, polarity (TPSA) between 20 and 130 $Å^2$, lipophilicity (XLOGP3) between -0.7 to +5.0, and flexibility not more than 9 rotatable bonds is suitable for oral bioavailability. Physicochemical property results indicate that two molecules (Entry 15 and 22) fulfill the criteria of drug likeness therefore selected for further studies. Molecule 15 offers H-bond interactions with Gln189, His164, Phe140 and Glu166. In addition, molecule 15 displayed hydrophobic interactions with Thr25, Thr26, Cys145, Gly143, Asn142, Leu141, Met165, His163, Cys44, His41, Met49 etc with $M^{pro}$ (Figure 3). Main protease of SARS-CoV-2 consists of three domains (I, II and III), the key residues Thr25, Thr26, Cys44, His41 and Met49 are of first domain, second domain contains Cys145, Gly143, Asn142, Leu141, Met165, His163 and Glu166 as key residues and in third domain Gln189 and Gln190 are present. Molecule 15 was displayed H-bond and hydrophobic interactions with the key residues of three domains. Figure 2, shows that molecule 15 was packed deeply inside the pocket by hydrophobic and H-bond interactions with the residues of domain first. Molecule (Entry 15) displayed intermolecular interactions with the key residues of domain I, II and III as shown in figure 2 (b).

The molecular docking of molecule (Entry, 15) was carried out with protein (PDB ID: 6M71), the intermolecular interactions like hydrogen-bond, Pi-Pi stacking and salt bridge were presented in figure 2 (b). Molecule displayed hydrogen bond interactions with Asp760, Lys621 and Lys551; salt bridge with Asp623, Arg553 and Asp760; Pi-Pi stacking with Tyr455 and Pi-cation bond formation with Arg553. In addition, molecule offered hydrophobic interactions with Arg624, Cys622, Pro620, Tyr619, Asp452 and Ala554. The molecular interactions of this molecule were compared with Remdesivir, it displayed hydrogen bond with Asp760, Asp618, and Lys621; Pi-Pi stacking with Asp623 and Pi-cation bond with Arg553 with protein (PDB ID: 6M71) (Figure 1 (b)). Molecule (entry 15) shows structural similarities with remdesivir including phenoxy and phosphate groups.

Structure activity relationship (SAR) study was performed to assign the role of scaffolds present in vitamin C based molecules. The lead molecule (Entry 15) contains three main functionalities, i.e., vitamin C on pocket 1, phenyl phosphate on pocket 2, and piperazine on pocket 3 as shown in figure 1. In the beginning, the role of phenyl phosphate (pocket 2) was studied; when docking of only vitamin C was carried out, it secured docking score -4.87 with protein (PDB ID: 6LU7) and -5.57 with protein (PDB ID: 6M71) highlighting the importance of phenyl phosphate group. Second variation was made on pocket 1, the replacement of vitamin C from a molecule keeping phenyl phosphate and piperazine groups as it is, the docking score further reduced to low value with both proteins. When vitamin C was replaced by dehydroascorbic acid, molecule offered lower docking score i.e. -4.721 and -5.37 respectively. Importantly, the replacement of vitamin C by nucleoside cytidine offered very best docking scores i.e. -8.167 (Entry 9) against protein Mpro and -5.949 against protein RdRp keeping 2 and 3 pockets constant. On the other hand, when pockets 1 and 3 were kept constant and a slight change was made in phenyl phosphate by substituting alkyl group on phenyl ring, the docking score found to be increased against both proteins. Interestingly, when pocket

3 was varied by substituting histamine and ester of glycine, best improvement in the docking score (i.e. -8.869 and -8.765) was observed (entries 3 & 4). Molecule 3 contains lactone ring in pocket 1, alkyl substituted phenyl phosphate group in pocket 2 and pocket 3 contains histamine. Molecule 4 possesses glycine ester in pocket 3 making no changes in pocket 1 and 2 respectively. The results clearly indicated the significance of natural vitamin C or cytidine, phenyl phosphate, piperazine or histamine or glycine ester in the pockets 1, 2 and 3 respectively. However, molecule 1 (entry 1) was shown to possess highest docking score in comparison to all other molecules in a series, that contains uridine nucleus in pocket 1, phenyl phosphate in pocket 2 and histamine in pocket 3, indicating the significance of nucleotide uridine.

Moreover, the ligand efficiency assessment study of fifteen molecules was carried out (Table 2) to find out the most suitable ligand to bind with protein. The ligand efficiency defines the ratio of affinity of ligand divided by the number of heavy atoms (nonhydrogen) in a molecule [Hopkins et al., 2004]. A lead molecule (Entry 15) has smaller size and follows Lipinski's rule of five. Ligand efficiency of this molecule is -0.215 with free energy of binding -41.93. As per the literature reports, the smaller molecules are more soluble and bioavailable and have fewer metabolic liabilities. A lead molecule possesses low molecular weight (MW= 400.32), good lipophilicity, high solubility, good gastrointestinal absorption, and more bioavailability properties.

Therefore, on the basis of molecular docking, ADMET properties, SAR analysis, and ligand efficiency measurement, molecule 15 was identified as the most suitable analog.

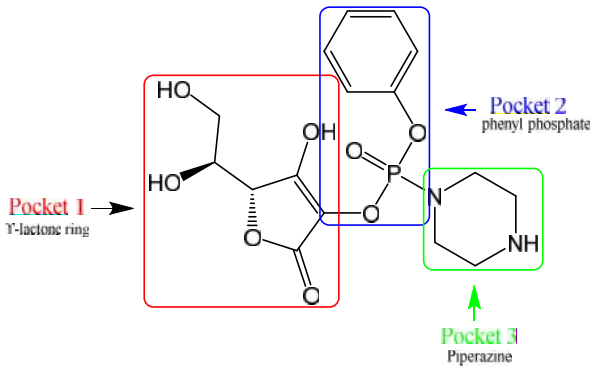


**Figure C**: Lead molecule (Entry 15, Table 3) with three main functionalities

**Table 1: Virtual Screening of Antiviral Drugs against SARS-CoV-2 with Protein 6LU7 and 6M71.**

| Entry | Antiviral Drugs | 6LU7(XP GScore kcal/mol) | Intermolecular interactions | 6M71(XP GScore kcal/mol) | Intermolecular interactions |
|---|---|---|---|---|---|
| **1** | Remdesivir | -6.974 | H-bond int.:Gln189, Thr190, Gly143, Glu166<br><br>Pi-Pi stacking: His41 | -4.942 | H-bond int.: Asp760, Asp618, Lys621; Pi-Pi stacking: Asp623 and<br><br>Pi-cation bond: Arg553 |
| **2** | Ritonavir | -6.273 | H-bond int.: Gln189, His164, Glu166<br><br>Pi-Pi stacking: His 41 | -2.134 | H-bond int.: Asp760, Tyr619, Lys621,<br><br>Pi-Pi stacking: Arg553, Lys798, Tyr455, |
| **3** | Paxlovid | -7.620 | H-bond int.:GLN189, His164, Thr26, Gly143 | -4.073 | H-bond Int.: Asp623, Lys621, Asp618, Arg553, Arg555 |
| **4** | Molnupiravir | -6.406 | H-bond int.: Gly143, Tyr54, His164 | -6.295 | H-bond int.: Asp760, Glu811, Lys798 |

**Table 2:** Intermolecular interactions of remdesivir analogs with protein (PDB ID: 6LU7)

| Entry | Molecules | Docking Score | Free Energy of Binding | Ligand Efficiency | Residue Interactions |
|---|---|---|---|---|---|
| 1 | 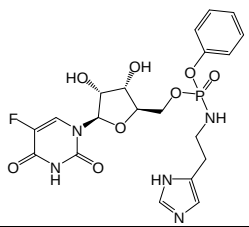 | -9.668 | -48.66837778 | -0.269 | H-bond: Glu189, Gly143, His41, Glu166 |

| | | | | | |
|---|---|---|---|---|---|
| 2 | 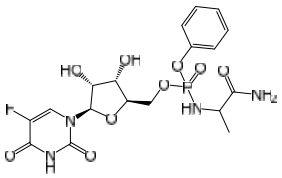 | -9.609 | -56.44769116 | -0.289 | H-bond: Glu189, Gly143, His41, Glu166 |
| 3 | 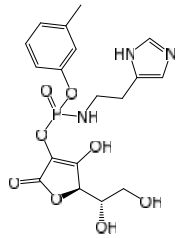 | -8.869 | -71.59398663 | -0.289 | H-bond: Thr26, Gly143, Glu166, Asn142 and salt bridge: His41 |
| 4 | 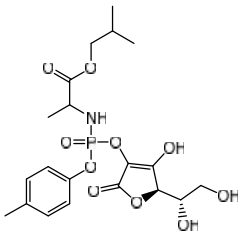 | -8.765 | -51.47183423 | -0.258 | H-bond: Gly143, Leu 141,Glu166, Phe140 and Asn142 |
| 5 | 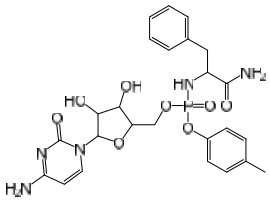 | -8.743 | -64.22656163 | -0.224 | H-bond: His41, His164 and Glu166 |
| 6 | 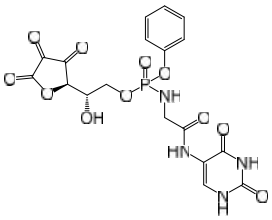 | -8.611 | -61.95687866 | -0.253 | H-bond:Thr26, Glu166, Asn142, Gly143 and His41 |
| 7 | 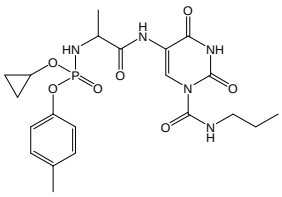 | -8.472 | -64.29758086 | -0.249 | H-bond:Gly143, Thr26, Glu166, Gln189 & His164 |
| 8 | 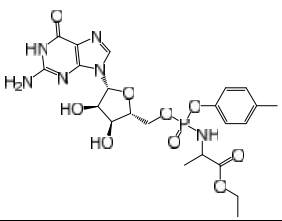 | -8.293 | -60.33501988 | -0.218 | H-bond: Glu166, Phe140 and GLY143 |

| | | | | | |
|---|---|---|---|---|---|
| 9 | 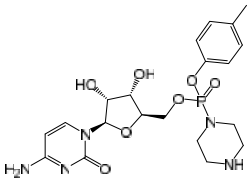 | -8.167 | -48.62512177 | -0.247 | H-bond: Thr26, His41, His164 and Glu166 |
| 10 | 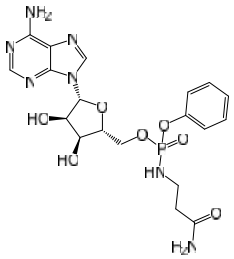 | -7.971 | -57.65639605 | -0.234 | H-bond:Glu189, Asn142, Leu167, Glu166 |
| 11 | 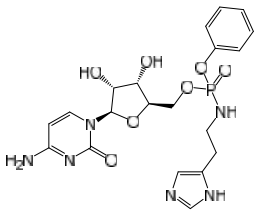 | -7.95 | -66.01291928 | -0.234 | H-bond: Asn142, His41 and Glu166 |
| 12 | 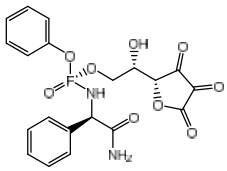 | -7.783 | -61.76857475 | -0.243 | H-bond: Gly143, Glu166, Leu141 |
| 13 | 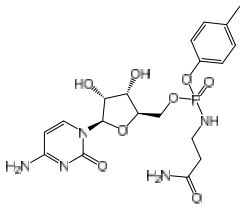 | -7.36 | -48.24965459 | -0.223 | H-bond: Glu166 and Cys145 |
| 14 | 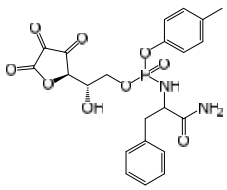 | -7.02 | -66.72081754 | -0.206 | H-Bond: Gly143, Asn 142, His41 (salt Bridge), Glu166 |
| 15 | 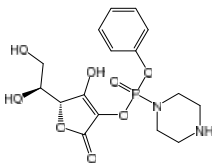 | -5.813 | -41.92730103 | -0.215 | H-bond:Gln189, His164, Glu166 and Phe140 |

**Table 3**: Intermolecular interactions of remdesivir analogs with protein (PDB ID: 6M71)

| Entry | Molecules | Docking Score | XP GScore (kcal/mol) | Residue Interactions |
|---|---|---|---|---|
| 16 | 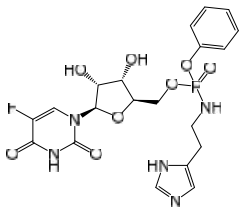 | -8.856 | -9.116 | H-bond: Glu811, Asp833, His816, Ser814, His810 |
| 17 | 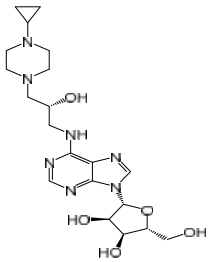 | -8.260 | -8.454 | H-bond: Asp760, Asp761, Asp623, Thr556, Arg555 |
| 18 | 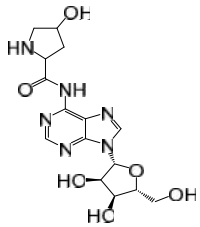 | -6.067 | -6.099 | H-bond: Asp760, Asp761, Asp623, Trp800, Lys798 |
| 19 | 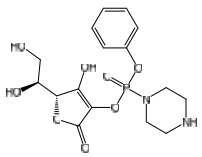 | -7.968 | -8.045 | H-bond: Asp760, Asp623, Lys621, Tyr455, Lys551, Arg553 |
| 20 | 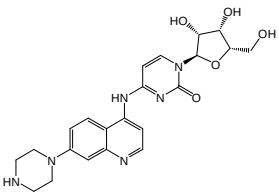 | -7.637 | -7.643 | H-bond: Asp760, Asp761, Glu811, Asp623, Thr556, Arg553 |
| 21 | 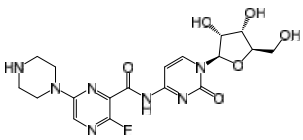 | -6.584 | -6.592 | H-bond: Asp760, Asp761, Lys621, Lys798, Ser795, Asp164, Phe793 |
| 22 | 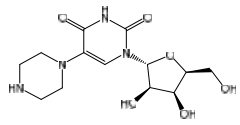 | -7.396 | -7.403 | H-bond: Asp761, His810, Trp617 |

| | | | | |
|---|---|---|---|---|
| 23 | 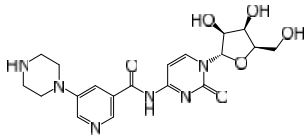 | -5.957 | -5.965 | H-bond: Asp760, Asp623, Tyr619, Arg553; Salt Bridge: Asp761 |
| 24 | 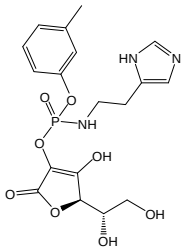 | -6.431 | -6.637 | H bond: Asp760, Tyr619, Cys622, Asp623, Tyr455 |
| 25 | 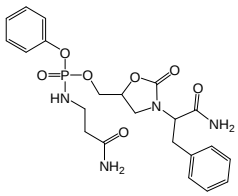 | -6.099 | -6.099 | H-bond: Asp760, Tyr619, Tyr455, Lys621, Asp623, Arg553 |
| 26 | 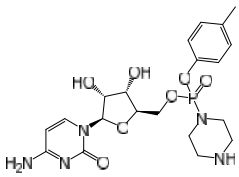 | -5.949 | -5.949 | H-bond: Asp760, Asp623, Tyr619, Cys622 |
| 27 | 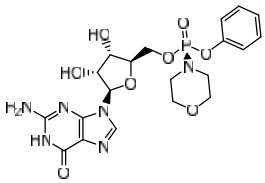 | -5.742 | -5.742 | H-bond: Asp760, Glu811, Trp617, Tyr619,Asp623, Arg553, Ser814 |
| 28 | 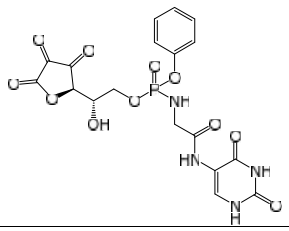 | -4.827 | -5.064 | H bond: Asp760, Tyr619, Lys621, Asp623, Arg624, Arg553, Arg555, Tyr455 |

**Table 4**: Physicochemical Properties of Remdesivir Analogs and Antiviral Drugs (Remdesivir and Paxlovid)[a]

| Entry | MW | nON | nOHNH | Nrot | TPSA | HIA | Caco-2 | Log $P_0$/w | BBB (abs.) | $LD_{50}$ | nVio |
|---|---|---|---|---|---|---|---|---|---|---|---|
| 1 | 512.41 | 10 | 6 | 10 | 191.85 | -0.9835 | -0.6663 | 2.65 | -0.7811 | 0.5540 | 3 |
| 2 | 488.36 | 11 | 5 | 9 | 205.01 | 0.5363 | -0.8016 | 1.20 | 0.5418 | 0.5923 | 1 |
| 3 | 439.36 | 9 | 5 | 10 | 177.12 | -0.9605 | -0.6678 | 1.64 | -0.6455 | 0.5730 | 1 |
| 4 | 491.41 | 10 | 4 | 11 | 190.28 | -0.7759 | -0.6864 | 1.77 | -0.7083 | 0.5707 | 1 |
| 5 | 559.51 | 10 | 5 | 11 | 211.06 | 0.7531 | -0.7504 | 1.51 | 0.5545 | 0.6135 | 2 |
| 6 | 496.32 | 12 | 5 | 11 | 232.86 | -0.9515 | -0.6823 | 0.40 | -0.8637 | 0.5437 | 1 |
| 7 | 493.45 | 8 | 4 | 13 | 170.43 | -0.5339 | -0.6189 | 2.41 | -0.6664 | 0.5870 | 1 |
| 8 | 552.47 | 12 | 05 | 11 | 222.95 | 0.6242 | -0.7174 | 1.60 | -0.5589 | 0.5165 | 2 |
| 9 | 482.45 | 9 | 4 | 7 | 175.79 | 0.5719 | -0.6386 | 1.81 | -0.5404 | 0.5794 | 1 |
| 10 | 493.41 | 11 | 5 | 10 | 219.77 | 0.6733 | -0.7274 | 1.89 | 0.5513 | 0.5391 | 1 |
| 11 | 493.43 | 9 | 6 | 10 | 197.90 | -0.9666 | -0.6673 | 0.32 | 0.5572 | 0.5628 | 1 |
| 12 | 462.35 | 10 | 3 | 10 | 181.13 | -0.5973 | -0.7197 | 0.08 | 0.5848 | 0.5706 | 1 |
| 13 | 483.41 | 10 | 5 | 10 | 211.06 | 0.6255 | -0.6841 | 1.40 | -0.5566 | 0.5669 | 1 |
| 14 | 490.40 | 10 | 3 | 11 | 181.13 | 0.5806 | -0.7246 | 1.39 | -0.7074 | 0.5823 | 1 |
| 15 | 400.32 | 9 | 3 | 7 | 155.01 | -0.8769 | -0.6722 | 1.74 | 0.7475 | 0.5832 | 0 |
| 16 | 512.41 | 10 | 6 | 10 | 191.85 | 0.9835 | 0.6663 | 2.65 | 0.7811 | 0.5540 | 3 |
| 17 | 450.51 | 9 | 6 | 8 | 153.46 | 0.6435 | -0.7438 | 2.19 | -0.6118 | 0.5260 | 2 |
| 18 | 381.36 | 8 | 5 | 5 | 159.23 | 0.5301 | -0.8343 | -0.26 | 0.6143 | 0.6170 | 1 |
| 19 | 400.32 | 9 | 3 | 7 | 155.01 | -0.8769 | -0.6722 | 1.74 | 0.7475 | 0.5832 | 0 |
| 20 | 456.39 | 6 | 6 | 6 | 150.83 | 0.8887 | -0.7174 | 1.52 | 0.6006 | 0.5815 | 2 |
| 21 | 452.42 | 10 | 5 | 6 | 179.54 | 0.6746 | -0.6734 | 0.87 | -0.5907 | 0.5686 | 1 |

| | | | | | | | | | | | |
|---|---|---|---|---|---|---|---|---|---|---|---|
| 22 | 329.33 | 6 | 5 | 3 | 144.63 | -0.6025 | -0.6956 | 0.99 | -0.7660 | 0.5836 | 0 |
| 23 | 433.44 | 8 | 5 | 6 | 166.65 | -0.6565 | -0.7047 | 0.74 | -0.5648 | 0.5867 | 1 |
| 24 | 439.36 | 9 | 5 | 10 | 177.12 | -0.9605 | -0.6678 | 1.64 | -0.6455 | 0.5730 | 1 |
| 25 | 490.45 | 8 | 3 | 13 | 173.09 | 0.6608 | -0.7397 | 2.37 | 0.5882 | 0.5980 | 1 |
| 26 | 482.45 | 9 | 4 | 7 | 175.79 | 0.5719 | -0.6386 | 1.81 | -0.5404 | 0.5794 | 1 |
| 27 | 508.42 | 11 | 4 | 7 | 197.09 | 0.9313 | -0.7056 | 1.47 | 0.7192 | 0.5589 | 2 |
| 28 | 496.32 | 12 | 5 | 11 | 232.86 | -0.9515 | -0.6823 | 0.40 | -0.8637 | 0.5437 | 1 |
| R | 602.58 | 12 | 4 | 14 | 213.36 | 0.8890 | -0.6599 | 3.52 | -0.7452 | 0.5357 | 2 |
| P | 499.53 | 8 | 3 | 11 | 131.40 | 0.9635 | -0.6684 | 2.17 | -0.7607 | 0.6008 | 0 |

[a]MW = molecular weight (g/mol); nON = no. of hydrogen bond acceptor; nOHNH = no. of hydrogen bond donors; Nrot = no. of rotatable bonds; HIA = human intestinal absorption; Caco-2 = colon carcinoma; TPSA = total polar surface area; Log Po/w = predicted octanol/water partition coefficient; $LD_{50}$ = oral rat acute toxicity; BBB = blood brain barrier; nVio. = no. of Lipinski violation; R = Remdesivir and P = Paxlovid

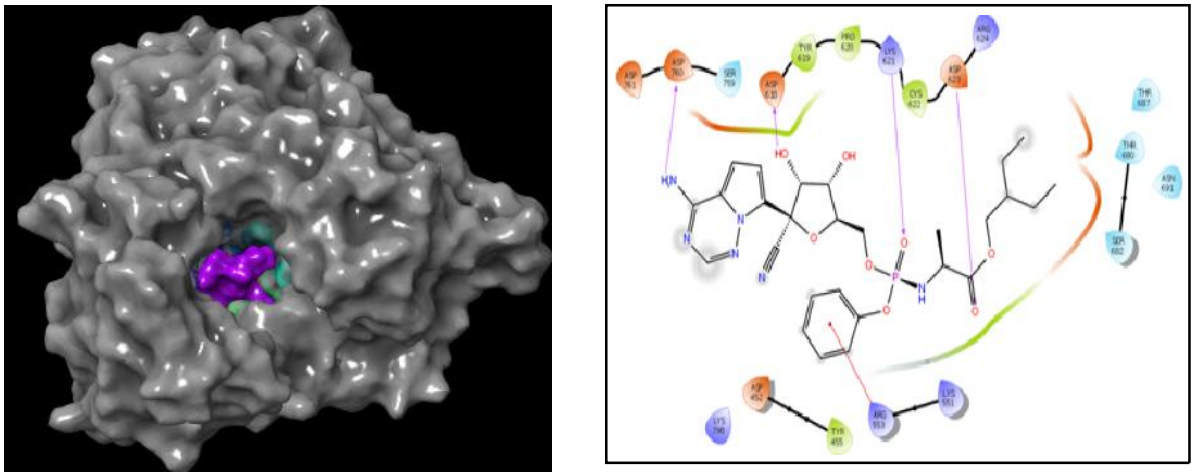

**Figure 1**: Remdesivir–RdRp docked complex, showing interactions with crystal structure 6M71(Pink colour) and surrounding residues.

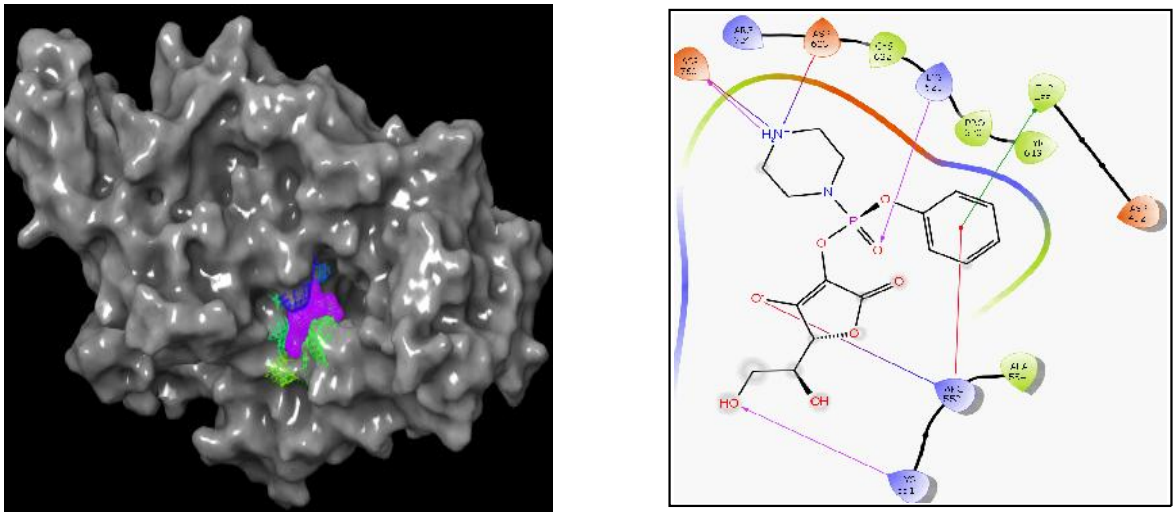

**Figure 2**: Compound 15–RdRp docked complex, showing interactions with crystal structure 6M71(Pink colour) and surrounding residues.

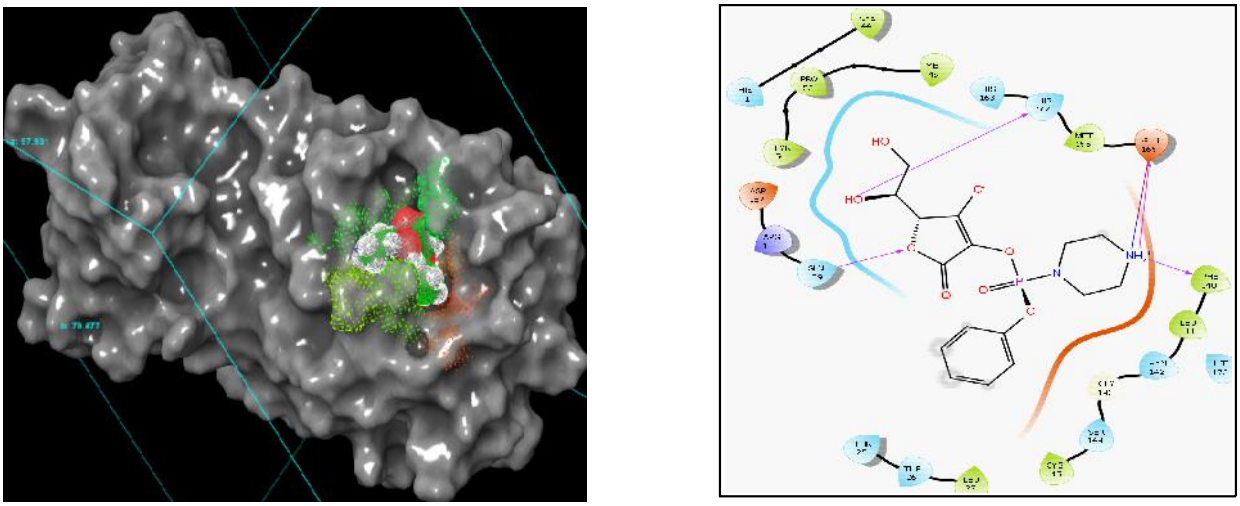

**Figure 3**: Compound 15–$M^{pro}$ docked complex, showing interactions with crystal structure 6LU7 (Green colour) and surrounding residues.

### 3.2. Protein Structure Analysis

Generally, protein structure study is rarely done, but its study provides very useful insight on the quality, topology, cavities, tunnels and clefts through which binding sights of protein-ligand interaction can be studied. The analysis is primarily image-based that includes protein secondary structure, protein-ligand, and protein-DNA interactions. PDBsum is a web server (http://www.ebi.ac.uk/pdbsum.) provides structural information on the proteins deposited in the Protein Data Bank (PDB) [Dias et al., 2019].

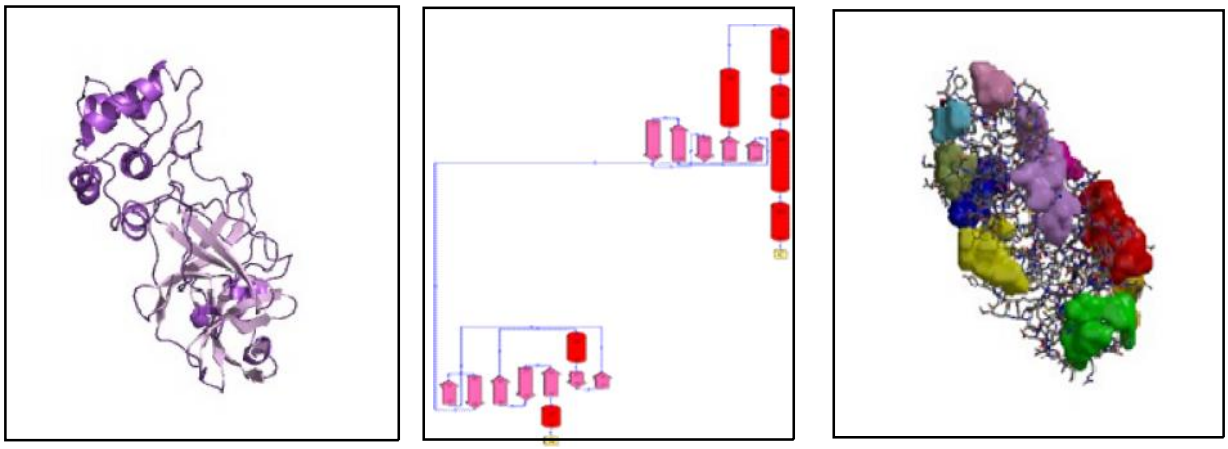

(a) (b) (c)

**Figure 4**: Showing protein chain of 6LU7 (a); its topology (b); and clefts in protein structure (c).

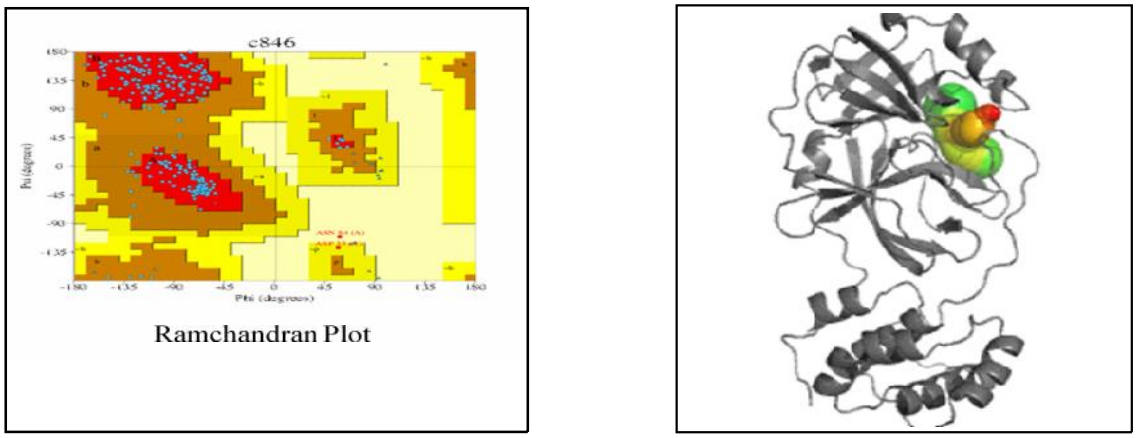


(d) (e)

**Figure 5**: Ramchandran plot of $M^{pro}$ (6LU7) (d) and tunnels in protein structure (e)

The statistical analysis of Ramchandran plot interprets that protein chain (a) contains 306 residues, of them, 240 residues were present in the most favoured regions, 24 were present in the allowed region and only one was present in the disallowed region. The protein chain contains 26 glycine residues and 13 proline residues. As per the reports, a good quality model expected to have over 90% residues in the most favoured regions. The present model contains 90.6% residues in the most favoured regions showing a good quality of protein.

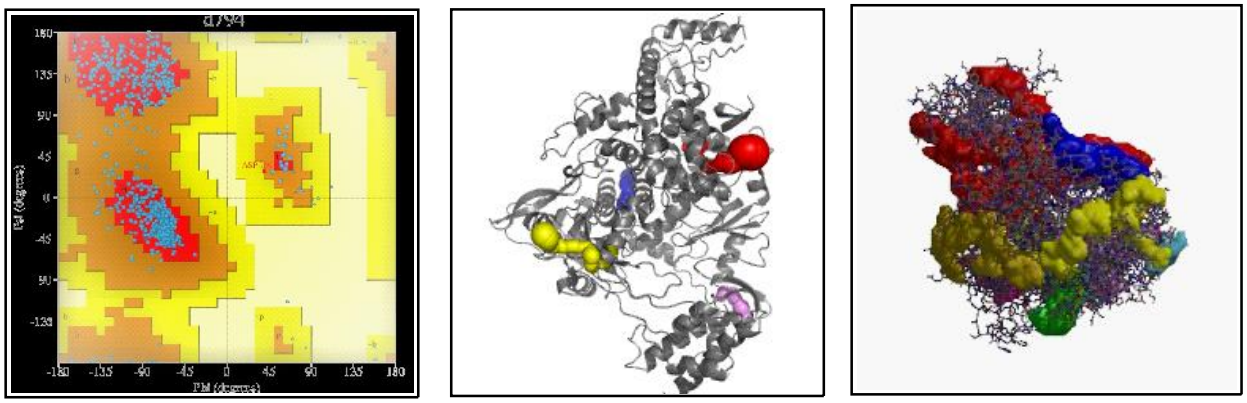

(f) (g) (h)

**Figure 6**: Ramchandran plot of ligand (15)-6m71complex (f); number of tunnels (g); and number of clefts (h)

Ramchandran plot statistics demonstrates that RdRp protein structure (PDB ID: 6M71) contains 859 residues out of that 708 (90.7%) residues are present in the most favoured region, 73 residues in the allowed regions and zero residues in the disallowed regions.

### 3.3. Protein and Solvent Dynamics

Detecting protein cavities, tunnels and clefts can provide valuable insight into protein properties including structure stabilization, internal hydration, substrate translocation and protein-ligand binding sites. A web based data set (PDBsum) was used for the analysis of pdb structures. A cleft is depression on the molecular surface called as pocket and works as binding site for ligands and other proteins. The proteins have internal cavities, termed as voids, which are isolated from the exterior environment. These are enzymatic reaction sites and constitutes highly controlled environment inside the protein. The proteins involved in transcription process have topological features including pores that are important for DNA binding. A pore is tunnel through a protein that connects an entry to an exit on the protein surface. Figure 4 (c) demonstrates that protein structure has four gaps red, purple, yellow and blue with types of residues. Protein structure contains three positive (H, K, R), two negative (D, E), four neutral (S, T, N, Q), five aliphatic (A, V, L, I, M), three aromatic (F, Y, W), proline, glycine and cysteine residues with volumes 11584.27, 3660.19, 3477.52 & 2670.89 respectively. Figure 5 (e) shows two tunnels in the protein structure of Mpro and Figure 6 (g) shows four tunnels at the active sites of RdRp, considered to be pathways for water, oxygen, proton and small molecules. Cleft analysis shows that RdRp structure consists of four gaps with volumes 1649.55, 2047.78, 1179.56 and 1088.86 respectively.

## Conclusion

The devastating impacts of COVID-19 pandemic intensely shook the human life with great economic losses. It has captured world's 80% population with huge mortality rate. The emerging variants like delta and omicron are also continuing to threat the human life around the world. In order to overcome the painful impacts of COVID-19, the rapid progress in the development of new vaccines and therapeutics is highly desirable. The protein targets are considerably helpful for the researchers to identify and design the potential drug candidates. In this context, virtual screening is one of the incredible approaches for structure-based designing of new molecules against a known target proteins.

In view of the above, we have carried out virtual screening of some approved antiviral drugs against main protease (Mpro) and RNA-depndent RNA polymerase (RdRp) protein. Our virtual docking results indicated that remdesivir, a known inhibitor of Ebola, has very good potential against both proteins of SARS-CoV-2, therefore selected as positive control for designing new drug candidates. Molecular docking of newly designed molecules was carried out and a total of 25 were identified with improved docking score with respect to remdesivir. In addition, molecule 15 was identified as a unique that completely follows Lipinski rule with best ADMET profile and molecular docking score. All identified molecules offer improved docking score than remdesivir and other approved antiviral drugs. Most of the molecules in a series possess very good ADMET profile with little violation of Lipinski rule. The intermolecular interaction and ADMET studies indicate that all identified molecules may play crucial role against SARS-COV-2 infection.

## Acknowledgments

This work was supported by Drug Discovery Programme, Government of India. We are very thankful to the whole team of drug discovery programme for guidance and making software available for the study. All the authors are very thankful to the Google for providing free online tools and servers for ADMET profile and protein analysis studies.

## References

Belete, T.M., 2021. Review on Up-to-Date Status of Candidate Vaccines for COVID-19 Disease. *Infect Drug Resist*. 14:151-161; https://doi.org/10.2147/IDR.S288877.

Biancatelli, R.M.L.C, Berrill, M., Marik, P.E., 2020. The antiviral properties of vitamin C. *Expert Rev Anti Infect Ther*. 18(2):99-101. doi: 10.1080/14787210.2020.1706483.

Carr, A. C., Maggini, S., 2017 "Vitamin C and Immune Function." *Nutrients.* 9(11): 1211. doi:10.3390/nu9111211.

Cheng, F., Li, W., Zhou, Y., Shen, J., Wu, Z., Liu, G., Lee, P.W., Tang, Y., 2012. admetSAR: a comprehensive source and free tool for assessment of chemical ADMET properties. *J Chem Inf Model*. 52(11):3099-105. doi: 10.1021/ci300367a.

Coronaviridae Study Group of the International Committee on Taxonomy of Viruses. 2020. The species Severe acute respiratory syndrome-related coronavirus: classifying 2019-nCoV and naming it SARS-CoV-2. *Nat Microbiol*. 5:536–544. doi:10.1038/s41564-020-0695-z.

Council, P., 2020. Lessons of past coronavirus pandemic. *Popul Dev Rev*. 633-637. Retrieved from https:/doi.org/10.1111/padr.12360

Daina, A., Michielin, O., Zoete, V., 2017. SwissADME: a free web tool to evaluate pharmacokinetics, drug-likeness and medicinal chemistry friendliness of small molecules. *Sci Rep*. 7, 42717. https://doi.org/10.1038/srep42717.

de Groot, R.J., Baker, S.C., Baric, R.S., Brown, C.S., Drosten, C., Enjuanes, L., et al. 2013. Middle East respiratory syndrome coronavirus (MERS-CoV): Announcement of the Coronavirus Study Group. *J Virol.*;87(14): 7790-2. doi:10.1128/JVI.01244-13.

Dehelean, C.A., Marcovici, I., Soica, C., Mioc, M., Coricovac, D., Iurciuc, S., Cretu, O.M., Pinzaru, I., 2021. Plant-Derived Anticancer Compounds as New Perspectives in Drug Discovery and Alternative Therapy. *Molecules. 26*, 1109. https://doi.org/10.3390/molecules26041109.

Dias, S., Simões, T., Fernandes, F., Martins, A.M., Ferreira, A., Jorge, J., et al., 2019. CavBench: A benchmark for protein cavity detection methods. *PLoS ONE.* 14(10): e0223596. https://doi.org/10.1371/journal.pone.0223596

Epik, Schrodinger Release 2020-1; Schrodinger, LLC: New York, 2020.

Food and Drug Administration. Fact sheet for healthcare providers: emergency use authorization for Evusheld (tixagevimab co-packaged with cilgavimab). 2021. Available at: https://www.fda.gov/media/154701/download.

Garvin, M.R., Prates, E.T., Pavicic, M., Jones, P., Amos, B.K., Geiger, A., Shah, M.B., Streich, J., Gazolla, J.G.F.M., Kainer, D., Cliff, A., Romero, J., Keith, N., Brown, J.B., Jacobson, D., 2020. Potentially adaptive SARS-CoV-2 mutations discovered with novel spatiotemporal and explainable AI models. *Genome Biol*. 21, 304. https://doi.org/10.1186/s13059-020-02191-0.

Gu, J., Korteweg, C., 2007. Pathology and pathogenesis of severe acute respiratory syndrome. *Am J Pathol.* 170(4):1136-47. doi: 10.2353/ajpath.2007.061088..

Hemilä, H. 2017. Vitamin C and Infections. *Nutrients*. 9(4):339. doi:10.3390/nu9040339.

Hopkins, A.L., Groom, C.R., Alex, A., 2004. Ligand efficiency: a useful metric for lead selection. *Drug Discov Today.* 9(10):430-1. doi: 10.1016/S1359-6446(04)03069-7.

https://www.worldometers.info/coronavirus/access on (15/03/ 2021), (n.d.).

Huremović, D., 2019. Brief History of Pandemics (Pandemics throughout History). *Psychiatry of Pandemics*. 7-35. doi:10.1007/978-3-030-15346-5_2.

Iftikhar, H., Ali, H. N., Farooq, S., Naveed, H., Shahzad-ul-Hussan, S., 2020. Identification of potential inhibitors of three key enzymes of SARS-CoV2 using computational approach. Comput Biol Med. 122: 103848.

Jin, Z., Du, X., Xu, Y., *et al.* 2020. Structure of $M^{pro}$ from SARS-CoV-2 and discovery of its inhibitors. *Nature* 582, 289-293. https://doi.org/10.1038/s41586-020-2223-y.

Kuhn, S.O., Meissner, K., Mayes, L.M., Bartels, K., 2018. Vitamin C in sepsis. *Curr Opin Anaesthesiol.* 31(1):55-60. doi: 10.1097/ACO.0000000000000549.

Kumar, S., Sharma, P.P., Shankar, U., Kumar, D., Joshi, S.K., Pena, L., Durvasula, R., Kumar, A., Kempaiah, P., *et al*. 2020. Discovery of New Hydroxyethylamine Analogs against $3CL^{pro}$ Protein Target of SARS-CoV-2: Molecular Docking, Molecular Dynamics Simulation, and Structure-Activity Relationship Studies. *J Chem Inf Model*. 60(12):5754-5770. doi: 10.1021/acs.jcim.0c00326.

Lan, J., Ge, J., Yu J., *et al.* 2020. Structure of the SARS-CoV-2 spike receptor-binding domain bound to the ACE2 receptor. *Nature.* 581, 215-220. https://doi.org/10.1038/s41586-020-2180-5.

LigPrep, Schrodinger Release 2020-1; Schrodinger, LLC: New York, 2020.

Lipinski, C.A., 2004. Lead- and drug-like compounds: the rule-of-five revolution. *Drug Discov Today Technol*. 1(4), 337–341.

Long, S.W., Randall, J.O., Paul, A.C., David, W.B., James, R.D., Maulik S., Marcus, N. et al. 2020. "Molecular architecture of early dissemination and massive second wave of the SARS-CoV-2 virus in a major metropolitan area." *MBio.* 11(6): e02707-20.

Lu, H., Stratton C.W., Tang, Y-W., 2020. Outbreak of pneumonia of unknown etiology in Wuhan, China: The mystery and the miracle. *J Med Virol*, 92:401-402. https://doi.org/10.1002/jmv.25678. b) Zhu, H., Wei, L., Niu, P., 2020. The novel coronavirus outbreak in Wuhan, China. *Glob Health Res Policy*, 5, 6. https://doi.org/10.1186/s41256-020-00135-6**.**

Maqbool, M. A., Aslam, M., Akbar, W., Iqbal, Z., 2017. Biological Importance of vitamins for human health: *A review / J. Agric. Basic Sci*., 2(3):2518-4210.

Pauling, L., 1971. The significance of the evidence about ascorbic acid and the common cold. *Proc Natl Acad Sci U S A.* 68:2678-81.

Pauling, L., Rath, M., An orthomolecular theory of human health and disease. 1991. *J Orthomol Med* 6:135-38.

Peck, K.M., Lauring, A.S., 2018. Complexities of viral mutation rates. *J Virol.* 92:e01031-17. https://doi.org/10.1128/JVI .01031-17.

Planas, D., Saunders, N., Maes, P., *et al.* 2022. Considerable escape of SARS-CoV-2 Omicron to antibody neutralization. *Nature* 602, 671–675. https://doi.org/10.1038/s41586-021-04389-z.

Prime, Schrodinger Release 2020-1: Schrodinger, LLC: New York, 2020.

Protein Preparation Wizard, Schrodinger Release 2020-1; Schrodinger, LLC: New York, 2020.

Rathor, L., 2021. Medicinal plants: A Rich Source of Bioactive Molecules Used in Drug Development. In: Mandal S. C., Chakraborth R., Sen S. (eds). Evidance Based Validation of Tradicinal Medicines. Springer, Singapore. https:/doi.org/10.1007/978-981-15-8127-4_10.

Richman, D.D., 2016. Nathanson, N., Antiviral Therapy. *Viral Pathogenesis*. 271-287. doi:10.1016/B978-0-12-800964-2.00020-3.

Singh, T.U., Parida, S., Lingaraju, M.C., Kesavan, M., Kumar, D., Singh, R.K., 2020. Drug repurposing approach to fight COVID-19. *Pharmacol Rep*.;72(6):1479-1508. doi:10.1007/s43440-020-00155-6.

Strasfeld, L., Chou, S., 2010. Antiviral drug resistance: mechanisms and clinical implications. *Infect Dis Clin North Am*. *24*(2), 413–437. https://doi.org/10.1016/j.idc.2010.01.001

van der Hoek, L., Pyrc, K., Jebbink, M.F., Vermeulen-Oost, W., Berkhout, R.J., Wolthers, K.C., Wertheim-van Dillen, P.M., Kaandorp, J., Spaargaren, J., Berkhout, B., 2004. Identification of a new human coronavirus. *Nat Med.* 10(4):368-73. doi: 10.1038/nm1024.

Veeresham, C., 2012. Natural products derived from plants as a source of drugs. *J Adv Pharm Technol Res.* 3(4):200-1. doi: 10.4103/2231-4040.104709. PMID: 23378939; PMCID: PMC3560124.

Wan, Y., Shang, J., Graham, R., Baric, R. S., Li, F., 2020. Receptor recognition by the novel coronavirus from Wuhan: an analysis based on decade-long structural studies of SARS coronavirus. *J. Virol.* https://doi.org/10.1128/JVI.00127-20.

Wu, K., Peng, G., Wilken, M., Geraghty, R. J., Li, F. 2012. Mechanisms of host receptor adaptation by severe acute respiratory syndrome coronavirus. *J. Biol. Chem*. 287, 8904–8911; b) Shang, J., Ye, G., Shi, K., Wan, Y. *et al.* 2020. Structural basis of receptor recognition by SARS-CoV-2. *Nature*, 581: 221-224.

Yin, W., Mao, C., Luan, X., Shen, D.D., Shen, Q., Su, H., Wang, X., Zhou, F., Zhao, W., Gao, M., Chang, S., Xie, Y.C., Tian, G., Jiang, H.W., Tao, S.C., Shen, J., Jiang, Y., Jiang, H., Xu, Y., Zhang, S., Zhang, Y., Xu, H.E., 2020. Structural basis for inhibition of the RNA-dependent RNA polymerase from SARS-CoV-2 by remdesivir. *Science* 368(6498):1499-1504. doi: 10.1126/science.abc1560.

| **Access this Article in Online** | |
|---|---|
| Quick Response Code | Website: www.ijarm.com<br>Subject: Molecular Docking |
| DOI:10.22192/ijamr.2022.09.10.001 | |

How to cite this article:
Babasaheb V Kendre, Pawan S Hardas, Rushikesh B Kendre. (2022). Discovery of New Remdesivir Analogs against Main Protease ($M^{pro}$) & RNA-Dependent RNA polymerase (RdRp) Targets of SARS-CoV-2: Molecular Docking, Physicochemical Properties, and Structure-Activity Relationship Studies. Int. J. Adv. Multidiscip. Res. 9(10): 1-22.
DOI: http://dx.doi.org/10.22192/ijamr.2022.09.10.001